

ASME Journal of Manufacturing Science and Engineering Online journal at:

https://asmedigitalcollection.asme.org/manufacturingscience



Nils Potthoff

Virtual Machining, TU Dortmund University, Otto-Hahn-Straße 12, 44227 Dortmund, Germany e-mail: nils.potthoff@tu-dortmund.de

Ankit Agarwal'

Department of Automotive Engineering, International Center for Automotive Research, Clemson University, Greenville, SC 29607 e-mail: agarwa3@clemson.edu

Florian Wöste

Virtual Machining, TU Dortmund University, Otto-Hahn-Straße 12, 44227 Dortmund, Germany e-mail: florian.woeste@tu-dortmund.de

Petra Wiederkehr

Virtual Machining, TU Dortmund University, Otto-Hahn-Straße 12. 44227 Dortmund, Germany e-mail: petra.wiederkehr@tu-dortmund.de

Laine Mears

Department of Automotive Engineering, International Center for Automotive Research, Clemson University, Greenville, SC 29607 e-mail: mears@clemson.edu

Evaluation of Contrived Wear Methodology in End Milling of Inconel 718

Tool wear plays a decisive role in achieving the required surface quality and dimensional accuracy during the machining of Inconel 718-based products. The highly stochastic phenomenon of tool wear, particularly in later stages, results in difficulty in predicting the failure point of the tool. The present research work aims to study this late-stage wear of the tool by generating consistent wear conditions and thereby decoupling the late-stage wear from the wear history. To do so, a multi-axis grinding operation is employed to create artificial tool wear that replicates the topology of natural wear occurring in the process. In order to evaluate the imitating ability of the proposed methodology, microscopic images in different wear states of naturally and contrived worn tools were analyzed. The methodology was validated by comparing the resulting process forces measured during end milling with the natural and contrived worn tool for different path strategies. Finally, a qualitative finite element (FE) analysis was conducted, and specific force coefficients for worn tool segments were determined through simulation.

[DOI: 10.1115/1.4062603]

Keywords: end milling, tool wear, decoupling wear, Inconel 718, machining processes, modeling and simulation

1 Introduction

Nickel-based superalloys (NBSAs) are a group of materials that exhibit high strength, ductility, and resistance to corrosion at elevated temperature and stress levels [1]. The superior properties of NBSAs make them an ideal option for manufacturing products with applications in aerospace, power-generation industries, and extremely challenging environments [2]. Milling is commonly employed to manufacture these products as it can produce intricate shapes with superior dimensional accuracy and higher productivity [3]. However, the properties of NBSAs mentioned earlier as functional benefits make them difficult to machine, leading to increased process forces and rapid tool wear. Such difficulty in the machining of NBSAs, especially Inconel 718 (IN718), results in the lower surface quality of the manufactured product [4], frequent tool change, and loss of productivity [5]. Therefore, to ensure the optimal use of the tool by the manufacturer, it is essential to predict tool wear within reasonable limits of accuracy.

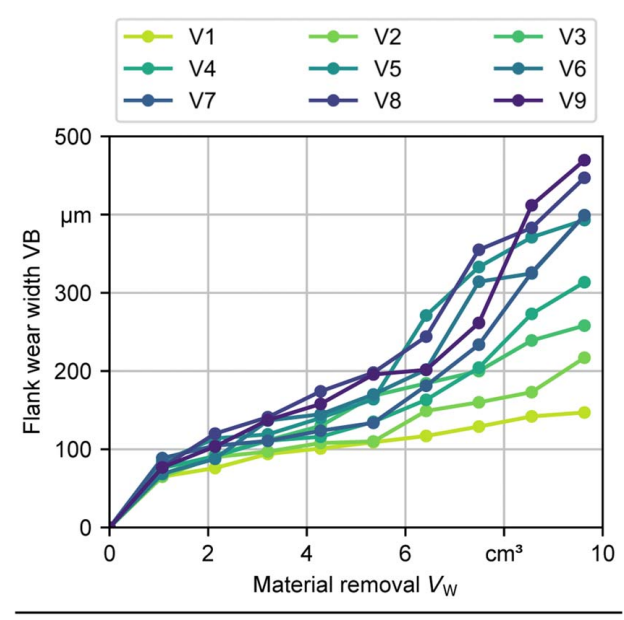
In the literature, several studies have been reported that aim to improve the productivity of IN718-based products by employing various toolpath strategies [6–8], optimizing cutting parameters [9-13], and developing models for predicting tool wear evolution [14-16]. Pleta et al. [6] applied trochoidal (i.e., epicyclcoidal) milling in the machining of IN718 and analyzed the effect of varying machining parameters such as cutting speed, feed, and depth of cut on material removal rate per unit of tool wear and cutting force dynamic response. The results were compared with conventional milling, and it was concluded that trochoidal milling has better productivity when the tool change is also considered, and the cutting force increases from the beginning to the end of the cut at a stable rate [7]. Sui et al. [8] generated a toolpath that combines corner-loop milling and clothoid curve transition strategies to optimize both the cutting force and dynamic characteristics of a machine tool during the machining of titanium alloys. The results showed reduced cutting force with improved stability and surface quality. Pleta et al. [9] identified the optimal values of cutting parameters to minimize process force and wear for IN718. The study also investigated the effect of these parameters on the depth of the machine-affected zone. Xavior et al. [10] applied the analysis of variance to evaluate the percentage influence of

¹Corresponding author.

Manuscript received January 29, 2023; final manuscript received May 20, 2023; published online June 7, 2023. Assoc. Editor: Vincent Wagner.

cutting parameters on flank wear and concluded that tool (insert) material is the most influential parameter. The literature also analyzed the effect of insert material [11], insert geometry [12], and insert coating [13] on tool wear and tool life while machining IN718. Furthermore, studies have been performed to investigate tool wear evolution in the machining of IN718 considering different cutting conditions and toolpath strategies [14]. Nouri et al. [15] monitored tool wear in real time and concluded that even under similar cutting conditions, the tool wear evolution varies and is a time-dependent stochastic process. Later, Niaki et al. [16] assessed the stochastic behavior of tool wear using Kálmán and Monte Carlo filters in another nickel-based difficult-to-machine material, i.e., Rene-108. From this background, the authors conclude that the stochastic nature of wear progression significantly affects the cutting, and it is variable enough not to be predictably repeatable. Therefore, a more controllable method is motivated.

In order to identify the stochastic behavior of tool wear in the machining of IN718, nine replicate tests were carried out in this study. Figure 1 shows the wear progression of these nine repeated tests and the process parameters used. A similar wear behavior could be observed in the initial stage $(V_w = 1 \text{ cm}^3)$, whereas the flank wear widths (VB) began to scatter more with increasing material removal. The progression of all experiments shows that after the initial wear phase, a region of inconsistent wear behavior is observed, making the study and prediction of tool wear difficult in the region of late wear. To overcome this problem, the phenomenon of tool wear in the later phase needs to be decoupled from the initial phase, requiring a different approach for analysis. Additionally, the studies related to tool wear analysis necessitate a significant number of tests and machining of a large volume of material. In the present study, the research in the phase of later tool wear will require machining a significant amount of material simply to produce such wear, resulting in cost-intensive and time-consuming experiments. Therefore, to decouple and analyze the late phase of the tool wear and avoid time-consuming and cost-intensive experiments for generating this wear, the tools can be artificially worn out to the desired level of wear widths in a more consistent manner than



Cutting velocity (v_c) : 40 m/min Feed per tooth (f_z) : 0.1 mm Material removal: 9.630 cm³ Depth of cut (a_p) : 1 mm Strategy: linear path milling Material: Inconel 718

Fig. 1 Variance of tool wear evolution of nine repeated experiments

through repeated machining. In this context, the present article aims to validate a methodology for generating artificial tool wear through a controlled multi-axis grinding operation. Therefore, the efficacy of the developed method was examined by comparing various direct (wear topography) and indirect quantitative (process forces, chip thickness, and force coefficients) attributes.

2 Methodology for Generating Tool Wear on Cutting Inserts

Tool wear during the machining of IN718 is stochastically influenced, as discussed in the literature [16]. To examine the wear behavior in detail, a methodology for artificially generating worn cutting inserts (contrived wear (CA)) with multi-axis positioning and a subsequent grinding operation is presented. For a comparative assessment of the contrived wear methodology, naturally worn (NW) cutting inserts were also generated. For the analysis, three representative wear states defined by a flank wear width of VB = 150 μ m, VB = 300 μ m, and VB = 450 μ m were generated on cutting inserts. The flank wear widths were selected such that they corresponded to three qualitative stages of tool wear, namely, initial stage, steady-state stage, and collapse stage. The wear widths were measured and analyzed using microscopic images of the cutting edges captured normally to the rake face using a Keyence VHX-950F microscope.

2.1 Generating Natural Tool Wear—Reference Inserts. In order to generate natural wear on the cutting inserts, linear path milling of IN718 was conducted using a five-axis machining center (DMG MORI DMU 50), as depicted in Fig. 2(a). The milling experiments were performed using a 2-flute indexable end-mill (CoroMill R390-016A16-11L) with a cutting diameter of $D=16\,$ mm, inserted with Sandvik Coromant R390-11 T3 08M-PM 1130 carbide inserts having multilayer ALTiCrN coating, a wiper edge length (b_s) of 1.2 mm, and a corner radius $r_c=0.8\,$ mm. Table 1 summarizes the machining parameter values. The flank wear widths were measured iteratively in between the machining passes to ensure that wear widths were achieved. The experiments were performed without the application of coolant.

During milling of IN718, it was observed that the abrasive and adhesive wear (initial and steady-state stages) superimposed up to tool failure (collapse stage) [14]. The microscopic images of inserts with different wear stages were also captured in the tool reference plane to measure the angle between the primary cutting edge and displaced tool corner, as shown in Fig. 2(b). An angle in the range of $13.73^{\circ} \pm 0.51$ was recorded for all inserts (cf. Ref. [18]).

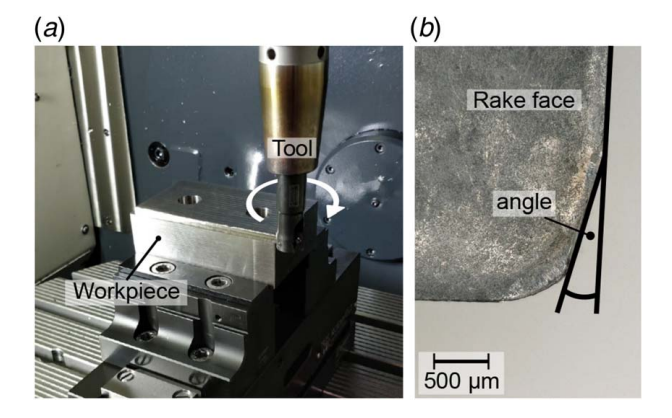


Fig. 2 (a) Experimental setup for generating naturally tool wear and (b) measurement of the angle between the major cutting edge and the displaced tool corner in the tool reference plane [17,18]

Table 1 Machining parameter values for generating natural tool wear

Cutting velocity (v_c) :	40 m/min
Feed per tooth (f_z) :	0.09 mm
Width of cut (a_a) :	1 mm
Depth of cut (a_p) :	1 mm

2.2 Generating Contrived Tool Wear. The contrived wear was then reproduced on a five-axis dressing machine (Geiger AP-800 Fusion) using a silicon carbide (SiC) grinding wheel with a resinoid bond. The SiC is a hard abrasive material commonly used in grinding wheels for dressing tools. The grinding wheel and tool were rotated in clockwise and counterclockwise directions to prevent the milling of the grinding wheel. The experimental setup for generating contrived tool wear is depicted in Fig. 3(a). To accurately generate the aforementioned flank wear widths representing three wear states, a camera system and an acoustic emission sensor were used to precisely position the grinding wheel and milling tool as shown in Fig. 3(b). The acoustic emission sensor detected the contact between the grinding wheel and the milling tool, which can be observed as a peak shown with arrows in Fig. 3(c).

After precise positioning, the flank wear widths were generated using a depth of cut of $a_p=1$ mm and width of cut of $a_e=5~\mu m$ per step feed. The parameter a_p was kept as it was used to generate the natural tool wear, while a_e was increased iteratively depending on the requirement for the flank wear width. The tool was rotated at a speed of $n_t=600~{\rm min}^{-1}$, while the speed of the grinding wheel was set to $n_g=1000~{\rm min}^{-1}$. The reproducibility of the proposed contrived wear methodology was validated by conducting three experiments under equal conditions. The flank wear widths were measured at each feed step up to a cumulative depth of $50~\mu m$ as shown in Fig. 3(d). The results show that consistent flank wear widths can be generated using the developed multi-axis contrived wear methodology as described in Ref. [18].

2.3 Analysis of Wear Topography. The wear topographies obtained using natural and contrived tool wear methodologies

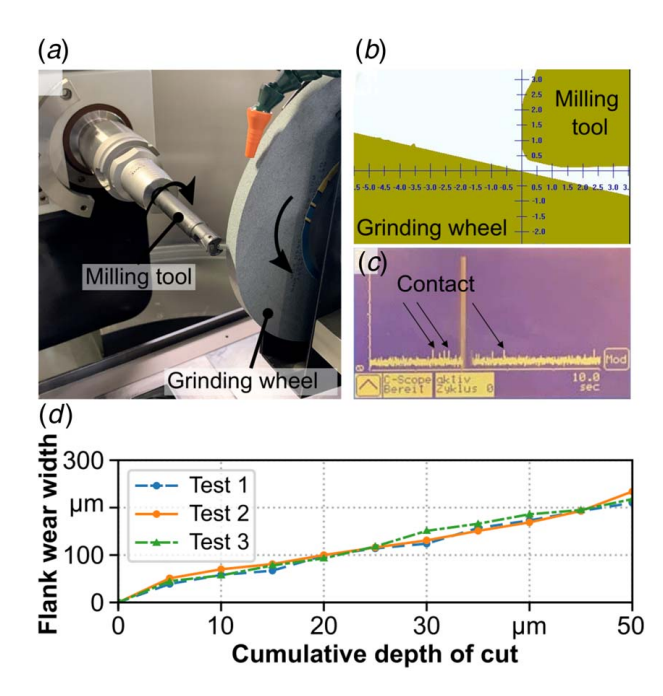


Fig. 3 (a) Experimental setup for generating contrived wear and (b) camera system for precise positioning. (c) Acoustic emission measurement and (d) reproducibility of contrived wear method (cf. Ref. [18]).

discussed earlier were qualitatively analyzed using scanning electron microscopy (SEM). In Fig. 4, SEM images of naturally and artificially worn inserts with wear widths of VB = 150 μ m, VB = 300 μ m, and VB = 450 μ m were compared. It can be seen that the shape of the flank wear region at VB = 150 μ m could be reproduced very effectively. However, the naturally worn tool showed a slight abrasive wear along the entire engagement width. Similarly, in the case of VB = 300 μ m, a comparable shape of the flank wear region was obtained, but smearing can be found on a naturally worn tool, which could not be reproduced effectively through simple grinding. Furthermore, at a flank wear width of VB = 450 μ m, a significant deviation in the in-depth topography was observed. This shows the need for further improvement of the methodology for generating contrived tool wear at higher flank widths.

3 Comparison of Process Forces in Linear and Trochoidal Cutting Paths

In order to validate the presented methodology for generating artificial tool wear, milling experiments with different path strategies—linear and trochoidal—were conducted with naturally and artificially worn inserts. For this purpose, cutting experiments were carried out on a five-axis machining center (*Deckel Maho DMU50 eVolution*). For the experiments with linear paths, a cutting speed of $v_c = 40 \, m/\text{min}$, a feed per tooth of $f_z = 0.1 \, \text{mm}$ and, width and depth of cut of $a_e = a_p = 1 \, \text{mm}$ were chosen. The process parameter values for trochoidal milling were adapted to ensure the comparability of both strategies. As described in Ref. [19], the trochoidal tool paths and, thus, the corresponding x-and y- coordinates were calculated as follows (Eq. (1)):

$$x_c = B\cos(\theta),$$

$$y_c = B\sin(\theta) + \frac{S_o \theta}{2\pi}$$
(1)

Here, the width (B) can be calculated as $B = (S_w - D)/2$ with the tool diameter of D = 16 mm and the slot width $S_w = 50$ mm. S_o represents the step over and is chosen as $S_o = 1$ mm, equivalent to the

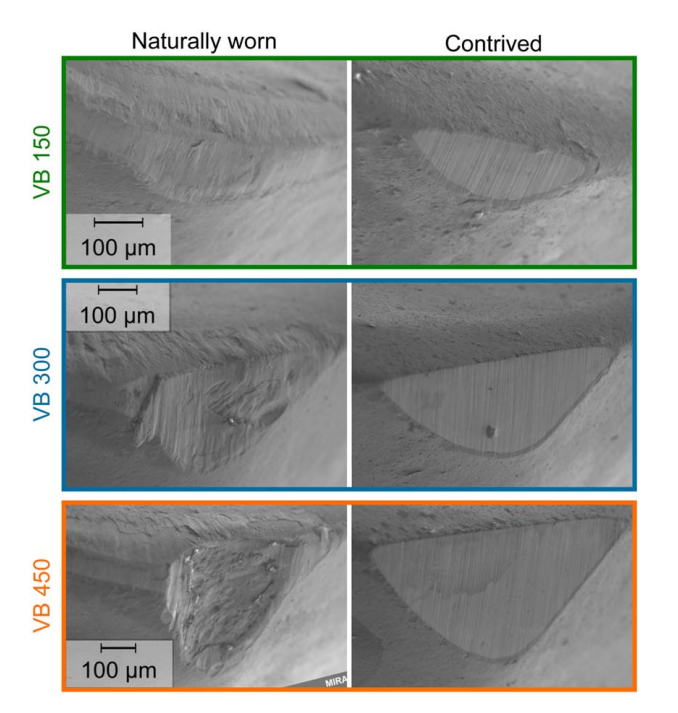


Fig. 4 SEM images of naturally and artificially worn inserts with different wear widths (VB = $150 \,\mu\text{m}$, VB = $300 \,\mu\text{m}$, VB = $450 \,\mu\text{m}$) (cf. Ref. [18])

width of cut of the linear machining strategy. The angle θ represents the path angle of the tool. Due to the superimposed rotation of the tool, a cutting speed of $v_c = 40~m/\text{min}$ was realized. The depth of cut remained the same $(a_p = 1~\text{mm})$. The experimental setup for the trochoidal path strategy is depicted in Fig. 5.

3.1 Dynamic Characterization of the Dynamometer. Force measurements are subjected to the dynamic transfer behavior of the dynamometer, which can cause significant measurement errors. This effect is particularly relevant in the case of periodic force excitations [20], which are a characteristic feature of milling processes. Therefore, an evaluation of the transfer behavior is essential for the interpretation of force measurements recorded during milling. To calculate the transfer function of the setup (dynamometer with workpiece), an impact hammer (Brüel & Kjær, type 8206-002) was used for excitation in x-, y-, and z- directions. The impact and the response of the dynamometer were recorded simultaneously. The fast Fourier transform was used to convert the signals from the time domain to a frequency domain representation. The transfer function was then described by the ratio of response and excitation (see Fig. 6(a)). The plot shows the average of ten transfer functions (dashed) and superimposed single measurements (gray). It can be seen that several eigenmodes were present, especially at frequencies over 1400 Hz. Consequently, periodic forces with frequencies in this range cannot be measured using this method without significant error. The frequency range of the transmission behavior that is relevant to the processes under consideration is shown in Fig. 6(b). It can be seen that for the tooth engagement frequency of $f_e = 26.5$ Hz and its harmonics, transfer behavior with a value close to 1 was present, indicating a sufficiently small measurement error.

3.2 Comparison of Process Force. As shown in Ref. [18] for an analogy test on an orthogonal cutting machine, a good accordance of the process forces for naturally worn and artificially worn inserts could be observed, especially for small flank wear widths. However, since a continuous cut was carried out, the methodology presented for decoupling tool wear needs to be separately validated in milling tests for different path strategies. In order to evaluate the occurring process forces, different natural and artificial wear states were initially prepared, as described in Sec. 2. For this purpose, flank wear widths of VB = 150 μ m, VB = 300 μ m, and VB = 450 μ m were generated, preparing three naturally worn and three artificially worn inserts for both linear and trochoidal machining. After a conditioning cut, only one path was milled to avoid the tool wear from progressing.

3.2.1 Linear Path Strategy. The resulting process forces in the x-, y-, and z- directions for linear milling are shown in Fig. 7. The left side shows the process forces for the contrived inserts for a

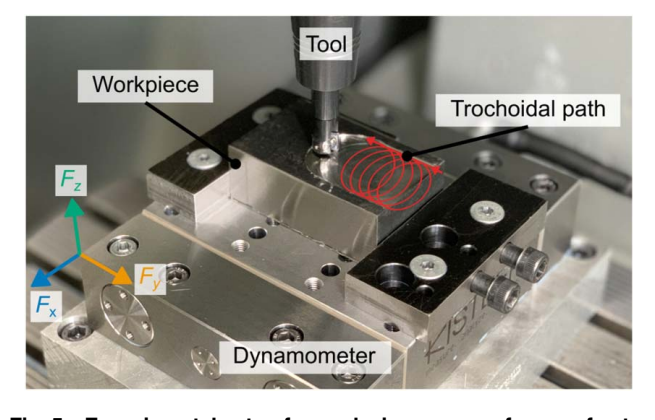


Fig. 5 Experimental setup for analyzing process forces of naturally and artificially worn inserts during trochoidal milling

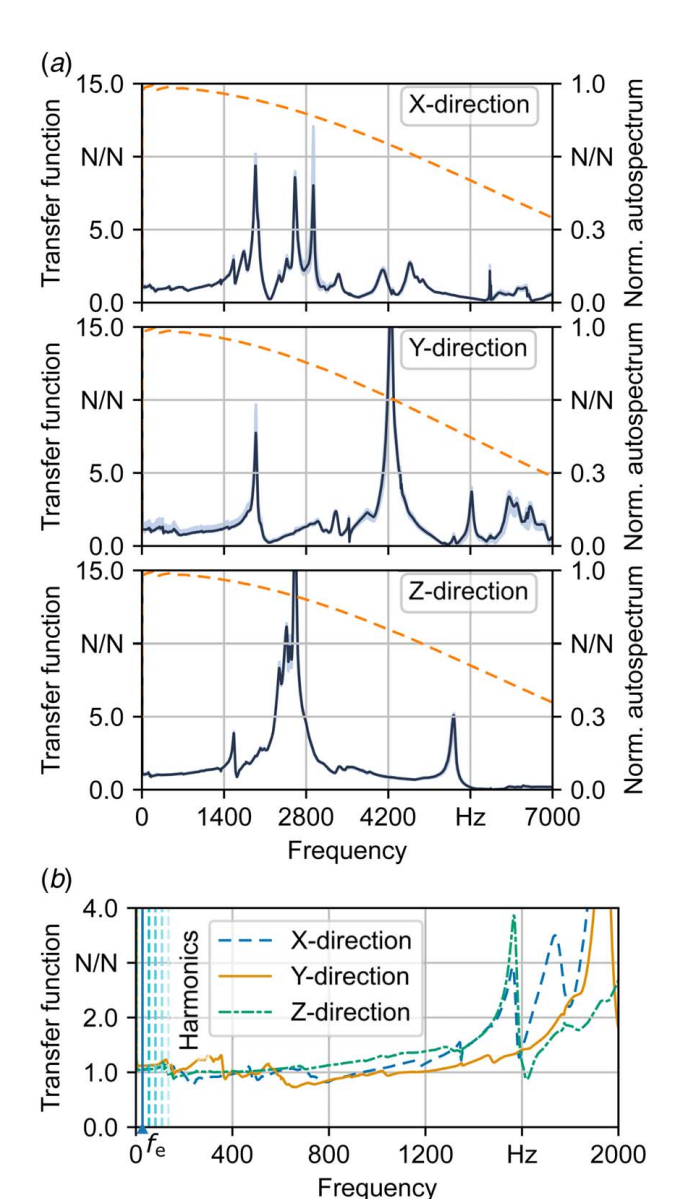


Fig. 6 (a) Transfer functions and the measurements (gray) in X-, Y- and Z-directions of the experimental setup with normalized autospectrum of the excitation force and (b) zoomed area of the transfer functions with tooth engagement frequency ($f_{\rm e}$) and its harmonics

half path. The right side shows the resulting process forces occurring with naturally worn inserts. It can be observed that the process forces generated with artificially worn inserts were slightly lower than the process forces of the naturally worn inserts (cf. Fig. 7—VB 150). The difference can be explained by the fact that only the major (circumferential) cutting edge was prepared when generating the artificial wear, whereas the natural tool wear also initially occurs along the corner radius, which leads to increased friction and, thus, to an increase of the process forces. The development of the process force for wear conditions VB 300 and VB 450 also showed good accordance. This is confirmed by the mean values of the process forces (cf. Table 2), which were determined by calculating the mean value of the peaks of all tooth engagements of a path milled. It can be seen that the mean values for the process forces in x- and y- directions differed by only $\approx 13\%$ and $\approx 11\%$, respectively. In the z-direction, the process forces of the naturally worn inserts were slightly higher with an average of ≈18%, which can be explained by the negligence of the tool wear on the minor cutting edge.

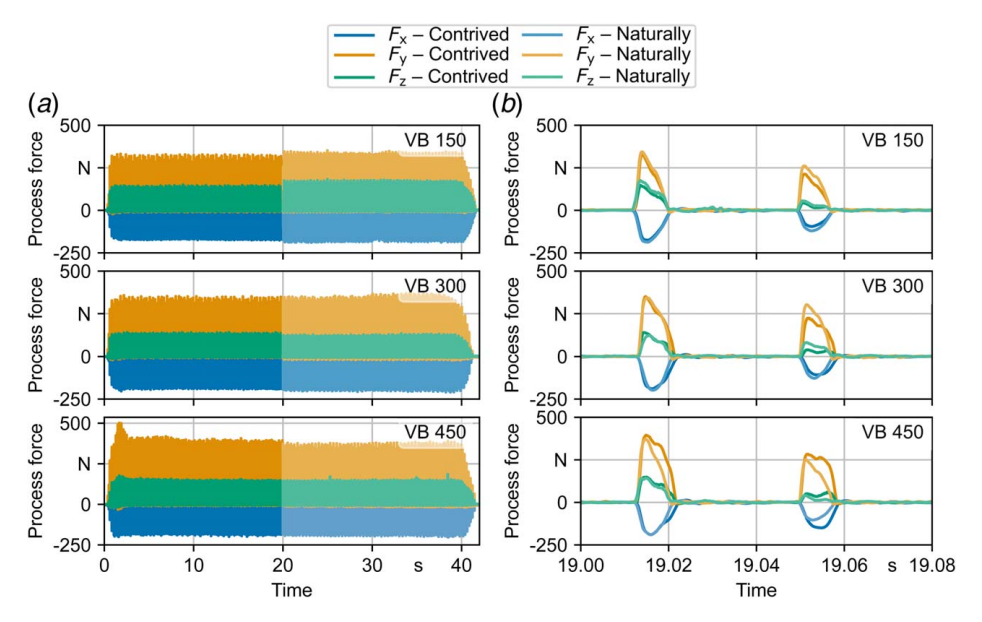


Fig. 7 (a) Process forces resulting from machining with a linear path with different wear states of contrived and naturally worn inserts and (b) a detailed view of two tooth engagements

A detailed analysis of the force progression of individual tooth engagements (see Fig. 7(b)) shows a high similarity, especially at the beginning of the cutting edge entry. A consistent force level was generally evident for different wear states, although slightly varying shapes emerged as the flank wear width increased. The deviation of the force level of two consecutive tooth engagements can be constituted by the runout error resulting from the modular tool system. However, the validation shows good accordance with the resulting process forces.

3.2.2 Trochoidal Path Strategy. Comparing the resulting process forces recorded during machining by means of a trochoidal path shows that the occurring tool wear could be well reproduced, especially for small flank wear width (VB 150), as depicted in Fig. 8. At higher flank wear width (VB 300 and VB 450), only a slight deviation could be detected, which confirms the results in Ref. [18]. Due to the varying process of force development in trochoidal milling, a detailed analysis of single-tooth engagements is necessary. Figure 8(b) shows a detailed view of the resulting forces. The process forces exhibited a good accordance regarding contrived and naturally worn states, even if slight deviations could be seen. In addition, vibrations were detected, which can negatively influence the process force. As well as for the process forces recorded during machining by means of the linear path strategy, slightly different shapes were noticeable. The results show that the presented methodology is suitable for generating artificial tool wear and, thus, decoupling tool wear from the milling process.

Table 2 Mean values of process forces of the linear path strategy with contrived and naturally worn inserts

	Flank wear width				
	VB 150	VB 300	VB 450		
$F_{x,CA}$	-132 N	-148 N	-170 N		
	272 N	287 N	347 N		
$F_{y,CA}$ $F_{z,CA}$	96 N	90 N	107 N		
$F_{x,NW}$	-152 N	-166 N	-150 N		
$F_{y,NW}$	305 N	333 N	314 N		
$F_{z,NW}$	117 N	107 N	97 N		

4 Finite Element Analysis of Digitized Inserts

For a more isolated analysis of the engagement with respect to cutting edge geometries of naturally worn and contrived inserts, a finite element analysis (FEA) was conducted. As described in Ref. [18], models for 2D FEA can be carried out using digitized cutting inserts. For this purpose, representative areas of a new, naturally worn, and artificially worn insert were digitized by using a confocal microscope. In order to investigate the same area of all three conditions, an alignment with the subsequent local best fit was carried out using the rake face and flank face. By segmenting the cutting edge, a profile could then be extracted that serves as the basis for the analysis. For the simulation, the profiles were extruded to a width of $w=40~\mu m$. Figure 9 summarizes the described method.

4.1 Finite Element Analysis of Naturally Worn and **Contrived Insert.** To compare the effect of contrived and naturally worn cutting edges on the resulting process forces, finite element analyses were conducted. For this purpose, an analogy model with only one linear cutting motion was set up to simulate orthogonal cuts. By considering orthogonal cutting processes, a more isolated analysis is possible due to simplified engagement conditions [21] compared to machining operations such as milling. The model was set up using the coupled Eulerian Lagrangian (CEL) method as implemented in the commercial software ABAQUS/ EXPLICIT. The applicability of the CEL method to model metal orthogonal cutting processes has been demonstrated in Ref. [22]. The tool, which was assumed to be rigid, was described by a Lagrangian reference and the workpiece by an Eulerian formulation using coupled temperature-displacement elements of the type EC3D8RT. To account for the influence of strain hardening, strain rate, and thermal softening on the material response of the workpiece, the constitutive law by Johnson and Cook was used, parameterized for IN718. The material and contact parameter values used as well as the defined spatial discretization of the tool and workpiece meshes are listed in Ref. [18]. In order to characterize the cutting edge with respect to the resulting cutting force, orthogonal cuts with seven different undeformed chip thicknesses (0.03 mm, 0.05 mm, 0.07 mm, 0.09 mm, 0.11 mm, 0.13 mm, and 0.15 mm) were simulated at a constant cutting velocity of $v_c = 40$ m/min. For reference, the profile of a new insert was also considered as part of the simulation experiments (see Fig. 10).

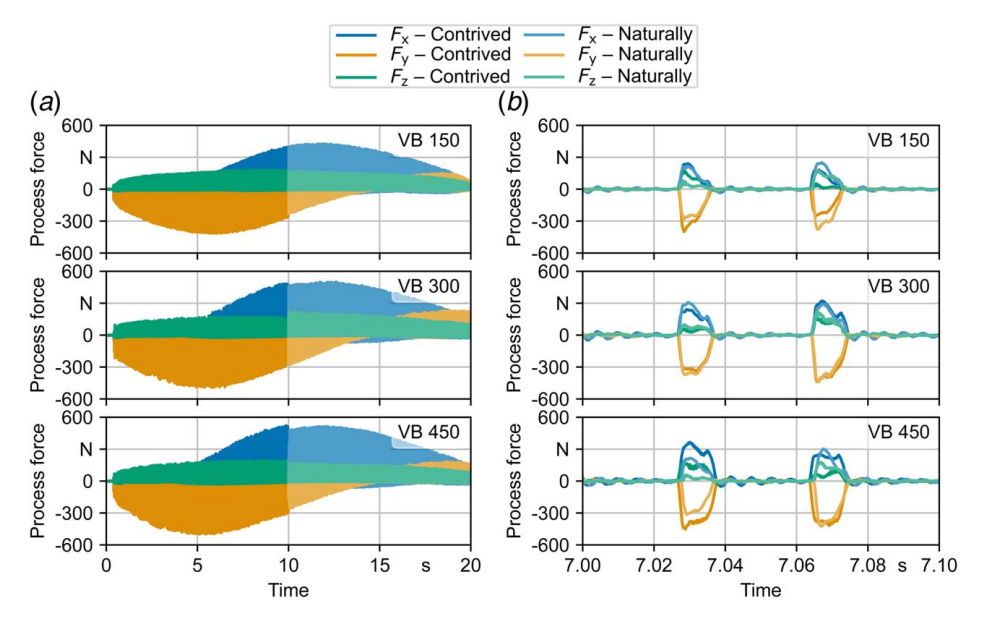


Fig. 8 (a) Process forces resulting from machining with a trochoidal path with different wear states of contrived and naturally worn inserts and (b) a detailed view of two tooth engagements

4.2 Calculation of Force Coefficients. By calculating specific cutting force coefficients in cutting (c) and normal direction (n) of the cutting edge, the load acting on the cutting edge can be characterized as a function of the undeformed chip thickness h_{cu} . For this purpose, the mean force values in the cutting and normal direction were calculated based on finite element (FE) simulations for each considered process configuration and normalized with respect to an undeformed chip area of 1 mm². This was carried out for two wear states (VB 150 and VB 300) of a naturally worn and a contrived insert, respectively, as well as for the profile of a new insert. The resulting specific forces are depicted in Figs. 11(a) and 11(b) as points. In general, an increase of specific forces can be observed with decreasing undeformed chip thicknesses as described in the literature [23]. This trend can be described using the empirical force model:

$$k_i(h_{cu}) = k_{i,1,1} h_{cu}^{-m_i}, i \in \{c, n\}$$
 (2)

which is, e.g., particularly suitable for the force modeling of machining processes with interrupted cuts such as milling [23,24]. The coefficients $k_{i, 1.1}$ and m_i were calibrated based on the specific forces determined for individual process configurations using FEA. The resulting curves representing these forces as a function of the undeformed chip thickness are depicted in Figs. 11(a) and 11(b) for different wear states in cutting and normal direction of the cutting edge. To determine, for instance, the process force F_i for different combinations of width of cut w and undeformed

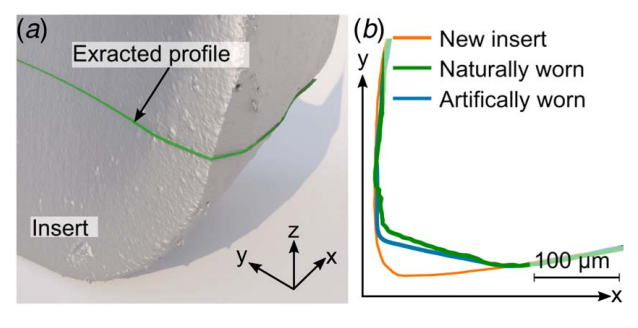


Fig. 9 Cutting edge segmentation for new, naturally worn and artificially worn inserts. (a) Exemplary profile extraction and (b) extracted profiles [18].

chip thicknesses h_{cu} based on such a model, Eq. (2) is inserted in Eq. (3)

$$F_i = w k_i(h_{\rm cu}) h_{\rm cu} \tag{3}$$

which is extended as follows (Eq. (4)) to obtain the correct unit [23]:

$$F_i = w \ k_{i,1.1} \ h_0 \left(\frac{h_{\text{cu}}}{h_0}\right)^{(1-m_i)}, \ h_0 = 1 \ \text{mm}$$
 (4)

The specific forces in the normal direction of the cutting edge k_n (see Fig. 11(a)) increased significantly for a wear state of VB 150 for both a NW and a CA insert compared to a new insert. It can be seen that the NW 150 and the CA 150 resemble each other closely, indicating a similar load acting in the normal direction. Likewise, both curves for a wear state of VB 300 are also very close to each other. The increase of the specific forces, however, is considerably larger than for VB 150. In general, the specific forces of the naturally worn inserts were slightly higher for the wear states considered, especially at smaller undeformed chip thicknesses. However, this shows that the load acting on a naturally worn cutting edge in the normal direction could be reproduced using the contrived wear methodology.

Since the wear affects primarily the force component in the normal direction, its influence on the forces in the cutting direction was comparatively small. It can be seen that with the exception of NW 150, a slight increase of the specific forces occurred for both wear conditions. In addition, the forces of the contrived inserts were in general minimally larger than those of the naturally worn inserts. The previously described significant increase of the specific force in the normal direction with progressing tool wear is reflected in the determined force coefficients listed in Table 3, especially with respect to a new insert. In particular, it can be seen from the values

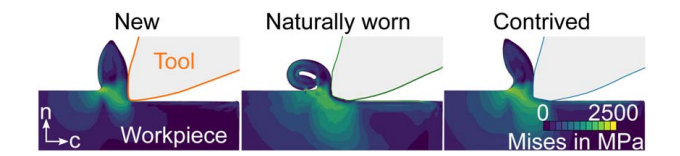


Fig. 10 Exemplary FE analysis of a naturally worn and contrived insert (VB 150 μ m) [18]

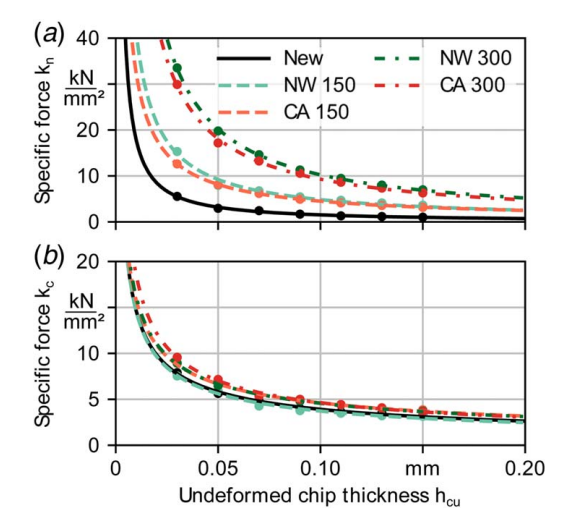


Fig. 11 Specific force coefficients $K_n(h_{\rm cu})$ and $K_c(h_{\rm cu})$ in (a) normal and (b) cutting directions of the cutting edge for new, naturally worn (NW), and contrived worn (CA) states based on results of the FEA

Table 3 Values of the determined force coefficients k_i and m_i based on the results depicted in Fig. 11

Туре	Cutting direction		Normal direction	
	$K_{c,1.1} \ (N/\text{mm}^2)$	m_c	$K_{n,1.1}$ (N/mm ²)	m_n
New	1043	0.57	129	1.07
NW150	950	0.59	567	0.93
CA150	1345	0.53	626	0.86
NW300	1290	0.55	1069	0.98
CA300	1156	0.60	1012	0.96

of $k_{n,1.1}$ and m_n for NW 150 and CA 150 as well as NW 300 and CA 300 that the load acting in the normal direction of the cutting edge of a naturally worn insert could be reproduced accurately with contrived inserts.

5 Conclusions

This article analyzed the stochastic influence in the later stage of tool wear and presents a methodology to generate artificial wear by multi-axis positioning of the tool with subsequent grinding in order to replicate the average experimental wear state. The methodology was experimentally validated for linear and trochoidal toolpath strategies for the machining of IN718. The transfer behavior was initially conducted to exclude dynamically induced errors. The following conclusions were drawn based on the outcomes of the present study:

- By using the proposed methodology for generating artificial tool wear, consistent wear conditions could be produced and the early and late stages of tool wear could be decoupled. The SEM images of the naturally and artificially worn tools showed a good agreement in the shape and microstructure of the wear topography. However, some deviation was observed in the case of higher flank width that needs further improvement.
- The resulting process forces obtained using naturally and artificially worn inserts showed similar force levels and shapes during linear and trochoidal milling, especially at lower flank wear widths. It can be inferred that the contrived wear methodology proposed in this article can effectively reproduce

- natural wear and avoid the requirement of time-consuming and cost-intensive experiments.
- The FE-based qualitative analysis of the chip geometry formation and resultant process forces of cutting edges of naturally and contrived worn tools showed a considerable influence. Also, this analysis can be further used to determine specific force coefficients.

In future investigations, a detailed analysis of the resulting topography of the artificially worn inserts compared to the naturally worn inserts will be conducted. Therefore, the progressive wear behavior of the inserts will be investigated with respect to induced residual stresses and thermal effects, which can lead to modification in the insert topology. In addition, the comparison of three-dimensional deviations will be executed using digitized inserts. Moreover, the presented methodology can be used to conduct a detailed analysis of worn cutting edges, from which a range of force coefficients can be determined allowing for a qualitative analysis of wear-dependent cutting edges.

Acknowledgment

The investigations are based on the research project "Stochastic Modeling of the Interaction of Tool Wear and the Machining Affected Zone in Nickel-Based Superalloys and Application in Dynamic Stability," which is kindly funded by the German Research Foundation (DFG—400845424) and the National Science Foundation (Grant No. 1760809). Any opinions, findings, and conclusions or recommendations expressed in this material are those of the authors and do not necessarily reflect the views of the National Science Foundation.

Conflict of Interest

There are no conflicts of interest.

Data Availability Statement

The authors attest that all data for this study are included in the paper.

References

- [1] Wu, B. H., Zheng, C. Y., Luo, M., and He, X. D., 2012, "Investigation of Trochoidal Milling Nickel-Based Superalloy," *High Speed Machining vol. 723* of *Materials Science Forum*, Z. Liu, Y. Wan, Q. Song, and Z. Shi, eds., TransTech Publ, Switzerland, pp. 332–336.
- [2] Thakur, A., and Gangopadhyay, S., 2016, "State-of-the-Art in Surface Integrity in Machining of Nickel-Based Super Alloys," Int. J. Mach. Tools Manuf., 100, pp. 25–54
- [3] Arunachalam, R., and Mannan, M., 2000, "Machinability of Nickel-Based High Temperature Alloys," Mach. Sci. Technol., 4(1), pp. 127–168.
 [4] Ulutan, D., and Ozel, T., 2011, "Machining Induced Surface Integrity in
- [4] Ulutan, D., and Ozel, T., 2011, "Machining Induced Surface Integrity in Titanium and Nickel Alloys: A Review," Int. J. Mach. Tools Manuf., 51(3), pp. 250–280.
- [5] Ezugwu, E., Wang, Z., and Machado, A., 1999, "The Machinability of Nickel-Based Alloys: A Review," J. Mater. Process. Technol., 86(1–3), pp. 1–16.
- [6] Pleta, A., Ulutan, D., and Mears, L., 2014, "Investigation of Trochoidal Milling in Nickel-Based Superalloy Inconel 738 and Comparison With End Milling," International Manufacturing Science and Engineering Conference, Detroit, MI, June 9–13, Vol. 45813, American Society of Mechanical Engineers, p. V002T02A058.
- [7] Pleta, A., and Mears, L., 2016, "Cutting Force Investigation of Trochoidal Milling in Nickel-Based Superalloy," Procedia Manuf., 5, pp. 1348–1356.
- [8] Sui, S., Li, Y., Shao, W., and Feng, P., 2016, "Tool Path Generation and Optimization Method for Pocket Flank Milling of Aircraft Structural Parts Based on the Constraints of Cutting Force and Dynamic Characteristics of Machine Tools," Int. J. Adv. Manuf. Technol., 85(5), pp. 1553–1564.
- [9] Pleta, A., Nithyanand, G., Niaki, F. A., and Mears, L., 2019, "Identification of Optimal Machining Parameters in Trochoidal Milling of Inconel 718 for Minimal Force and Tool Wear and Investigation of Corresponding Effects on Machining Affected Zone Depth," J. Manuf. Process., 43(Part B), pp. 54–62.
- [10] Xavior, M. A., Manohar, M., Jeyapandiarajan, P., and Madhukar, P. M., 2017, "Tool Wear Assessment During Machining of Inconel 718," Procedia Eng., 174, pp. 1000–1008.

- [11] Cantero, J., Díaz-Álvarez, J., Miguélez, M., and Marín, N., 2013, "Analysis of Tool Wear Patterns in Finishing Turning of Inconel 718," Wear, 297(1-2), pp. 885-894
- [12] Altin, A., Nalbant, M., and Taskesen, A., 2007, "The Effects of Cutting Speed on Tool Wear and Tool Life When Machining Inconel 718 With Ceramic Tools," Mater. Des., 28(9), pp. 2518–2522.
- [13] Ucun, I., Aslantas, K., and Bedir, F., 2013, "An Experimental Investigation of the Effect of Coating Material on Tool Wear in Micro Milling of Inconel 718 Super Alloy," Wear, 300(1–2), pp. 8–19.
- [14] Potthoff, N., and Wiederkehr, P., 2021, "Fundamental Investigations on Wear Evolution of Machining Inconel 718," Procedia CIRP, 99, pp. 171–176.
- [15] Nouri, M., Fussell, B. K., Ziniti, B. L., and Linder, E., 2015, "Real-Time Tool Wear Monitoring in Milling Using a Cutting Condition Independent Method," Int. J. Mach. Tools Manuf., 89, pp. 1–13.
- [16] Niaki, F., Ulutan, D., and Mears, L., 2015, "Stochastic Tool Wear Assessment in Milling Difficult to Machine Alloys," Int. J. Mechatron. Manuf. Syst., 8(3–4), pp. 134–159.
- [17] Grimm, T., Potthoff, N., Kharat, N., Mears, L., and Wiederkehr, P., 2021, "Development of a Contrived Tool Wear Method in Machining," Proceedings of ASME International Mechanical Engineering Conference and Exposition, Virtual, Online, Nov. 1–5.

- [18] Potthoff, N., Agarwal, A., Wöste, F., Liß, J., Mears, L., and Wiederkehr, P., 2022, "Experimental and Simulative Analysis of an Adapted Methodology for Decoupling Tool Wear in End Milling," Manuf. Lett., 33(Supplement), pp. 380–387
- [19] Bergmann, J. A., Potthoff, N., Rickhoff, T., and Wiederkehr, P., 2021, "Modeling of Cutting Forces in Trochoidal Milling With Respect to Wear-Dependent Topographic Changes," Prod. Eng., 15(6), pp. 761–769.
- [20] Ricardo Castro, L, Viéville, P., and Lipinski, P., 2006, "Correction of Dynamic Effects on Force Measurements Made With Piezoelectric Dynamometers," Int. J. Mach. Tools Manuf., 46(14), pp. 1707–1715.
- [21] Arrazola, P., Özel, T., Umbrello, D., Davies, M., and Jawahir, I., 2013, "Recent Advances in Modelling of Metal Machining Processes," CIRP Ann., 62(2), pp. 695–718.
- [22] Ducobu, F., Arrazola, P.-J., Rivière-Lorphèvre, E., de Zarate, G. O., Madariaga, A., and Filippi, E., 2017, "The CEL Method as an Alternative to the Current Modelling Approaches for ti6al4v Orthogonal Cutting Simulation," Procedia CIRP, 58, pp. 245–250.
- [23] Kienzle, O., 1952, "Die bestimmung von kräften und leistungen an spanenden werkzeugen und werkzeugmaschinen," VDI-Z, 94(11), pp. 299–305.
 [24] Bouzakis, K.-D., Methenitis, G., and König, W., 1985, "Determination of the
- [24] Bouzakis, K.-D., Methenitis, G., and König, W., 1985, "Determination of the Values of the Technological Parameters Which Are Used to Describe the Time Course of Cutting Force Components in Milling," CIRP Ann., 34(1), pp. 141–144.